J Clust Sci (2017) 28:529–550
DOI 10.1007/s10876-016-1129-1

ORIGINAL PAPER

Towards Bio-Encapsulation of Chitosan-Silver Nanocomplex? Impact on Malaria Mosquito Vectors, Human Breast Adenocarcinoma Cells (MCF-7) and Behavioral Traits of Non-target Fishes

Kadarkarai Murugan[1,2] · Anitha Jaganathan[1] · Udaiyan Suresh[1] · Rajapandian Rajaganesh[1] · Sudalaimani Jayasanthini[1] · Akon Higuchi[3] · Suresh Kumar[4] · Giovanni Benelli[5]

Received: 3 November 2016 / Published online: 28 November 2016

Abstract In this study, we synthesized and bio-encapsulated a chitosan-silver nanocomplex (Ch-AgNPs), characterizing it by UV–Vis spectroscopy, FTIR, EDX, SEM, XRD and Zeta potential analyses. The bio-encapsulated chitosan-Ag nanocomplex (BNC) was efficient as scavenger of free radicals (DPPH and ABTS), if compared to Ch-AgNPs. In toxicity assays against breast cancer cells (MCF-7) the BNC triggered apoptotic pathways, leading to a decline of MCF-7 cell viability with IC_{50} of 17.79 µg/mL after 48 h of exposure. LC_{50} of BNC on *Anopheles stephensi* ranged from 54.65 (larva I), to 98.172 ppm (pupa) while Ch-AgNPs LC_{50} ranged from 4.432 (I) to 7.641 ppm (pupa). In the field, the application of Ch-AgNP ($10 \times LC_{50}$) lead to *A. stephensi* larval reduction to 86.2, 48.4 and 100% after 24, 48, and 72 h, while the BNC nanocomplex exhibited 68.8, 36.4 and 100% larval reduction, respectively. Both Ch-AgNPs and the BNC reduced longevity and fecundity of *A. stephensi*. As regards to non-target effects on fish behavioral traits, in standard conditions, *Poecilia reticulata* predation on *A. stephensi* larvae was

✉ Giovanni Benelli
benelli.giovanni@gmail.com

[1] Division of Entomology, Department of Zoology, School of Life Sciences, Bharathiar University, Coimbatore 641046, Tamil Nadu, India

[2] Department of Zoology, Thiruvalluvar University, Serkkadu, Vellore 632115, Tamil Nadu, India

[3] Department of Chemical and Materials Engineering, National Central University, Taoyuan 32001, Taiwan

[4] Department of Medical Microbiology and Parasitology, Universiti Putra Malaysia, 43400 Serdang, Slangor, Malaysia

[5] Department of Agriculture, Food and Environment, University of Pisa, via del Borghetto 80, 56124 Pisa, Italy

70.25 (II) and 46.75 larvae per day (III), while post-treatment with sub-lethal doses of BNC, predation was boosted to 88.5 (II) and 70.25 (III) larvae per day.

Keywords Biosafety · Biological control · MCF-7 · Nanoparticle stability

Introduction

Arthropods are dangerous vectors of deadly diseases, which may hit as epidemics or pandemics in the increasing world population of humans and animals [11, 12, 47]. Mosquitoes (Diptera: Culicidae) are vectors of a wide number of diseases of public health and veterinary importance, including malaria, filariasis, setariosis, Japanese encephalitis, dengue, chikungunya, and even Zika virus, as recently outlined by the outbreaks in the Americas and in the Pacific [10, 13].

Malaria directly and indirectly affects the health and wealth of humans, as well as nations. Indeed, malaria is identified both as a disease associated with and a cause of poverty [29]. *Plasmodium* parasites causing malaria are vectored by *Anopheles* mosquitoes, with special reference to *Anopheles stephensi*. There were about 198 million cases of malaria in 2013 and an estimated 584,000 deaths. However, malaria mortality rates have fallen by 47% globally since 2000 and by 54% in the African region. Most deaths occur among children living in Africa, where a child dies every minute from malaria. Malaria mortality rates among children in Africa have been reduced by an estimated 58% since 2000 [77].

The effective control of malaria mosquito vectors is the basic requirement for planning a reliable management of the malaria burden. Indoor and outdoor residual spraying has played an important role in reducing vector borne disease transmission and morbidity and mortality in various endemic settings [56]. However, the efficacy of chemical pesticides currently used is declining rapidly, due to the development of resistance in many mosquito species and strains, thus novel eco-friendly pesticides are required [5, 6].

Nanoparticles of biological origin are of great interest due to their unusual optical [36], chemical [38], photoelectrochemical [73], and electronical [40] activities. Biofabricated nanoparticles can be used as novel pesticides, antioxidants, sensors [78], pesticides [7, 8], drug carriers [9, 53]. In recent years, it has been emphasized the application of nanotechnology in Integrated Pest Management and parasitology [5].

Technologies like encapsulation and controlled release system have, therefore, revolutionized the application of biocides. The nano-encapsulation-based formulations comprises nanoparticles with size rage of 120–250 nm being more effectively water soluble if compared to the some of the existing pesticides. Using nano- and micro-encapsulation fabrication technique, capsules with well-controlled size and shape, finely tuned wall thickness, and variable wall composition have been produced. Thus, these formulations can be applied for the controlled release of encapsulated substances [26], which allow using them against vectors, and targeted delivery of biologically active and medical substances to selected organisms

[20, 82]. The nanoencapsulated pesticides can easily be incorporated in different media and used as creams, gels and liquids. Therefore, the targeted organisms can more rapidly take them up. Furthermore, the encapsulated pesticides have more shelf life and killing capacity if compared to the respective chemically optimized ones [55].

Among the different nanoparticles investigated for biomedical and agricultural purposes, silver nanoparticles (AgNP) have received significant consideration because they are effective antimicrobial, anticancer and photocatalytic agents [30]. The use of AgNP as drug carriers is a promising method for the treatment of a wide variety of diseases, including malaria, dengue, cancer and multidrug resistant bacteria [7–9]. AgNP have emerged as nano-gels/sprays for use in cosmetic and drug industries as well as nanocomposite for mosquitocidal purposes [45, 46, 68]. To further improve the mechanical properties and functionalities of nanoparticles, the encapsulation of nanomaterials has been adopted using polymeric substances [18].

Chitosan (Ch), a polysaccharide of animal origin [14], is a natural, biodegradable polysaccharide polymer, which is the major structural component in the exoskeleton of crabs, lobsters, shrimps, prawns, crayfish and insects [15]. Chitosan is a semi-crystalline polymer and crystallinity plays an important role in its adsorption efficiency [76]. It consists of a β-(1,4)-linked-D-glucosamine residue with the amine groups randomly acetylated [66]. The amine and –OH groups endow chitosan with many special properties, making it applicable in many areas and easily available for chemical reactions [64, 71]. Because of its advantageous properties including biodegradability, biocompatibility, anti-bacteria and non-toxicity, chitosan can be used in the fields of food processing, pharmaceuticals, cosmetics, biomaterials and agriculture [60, 75]. In vitro, chitosan-fabricated nanoparticles exerted cytotoxicity against colon cancer cells (Calo320), gastric cancer cells (BGC823), liver cancer cells BEL7402 [57] and HepG2 [79].

To the best of our knowledge, no efforts have been conducted to shed light on bioactivity of bio-encapsulated chitosan-fabricated nanoparticles against mosquito vectors of medical and veterinary importance [9].

Therefore, here we attempted the bio-encapsulation of chitosan-Ag nanocomplex, in order to provide a new class of collagen/polymer-based biomaterials with good biological properties. We combined chitosan with a noble metal, such as Ag [47], which is then encapsulated by a polymer coat evaluating its potential against parasites and vectors.

Bio-encapsulated chitosan-Ag nanocomplex was characterized by UV–Vis spectroscopy, Fourier Transform Infrared (FTIR) spectroscopy, X-ray diffraction (XRD) analysis, EDAX and SEM. Then, the bio-encapsulated chitosan-Ag nanocomplex was evaluated in comparison with classic chitosan-synthesized Ag nanoparticles testing: (i) the toxicity against the malaria vector *A. stephensi*, both in laboratory and in the field. (ii) the free radical scavenging potential on DPPH and ABT, (iii) the cytotoxicity via apoptosis-triggering mechanisms on breast cancer cells (MCF-7), (iv) the impact of sub-lethal doses of nano-products on the predation

efficiency of non-target larvivorous fishes *Poecilia reticulata* predating anopheline larvae.

Materials and Methods

Chemicals

Silver nitrate and DPPH were purchased from Sigma-Aldrich (Mumbai, India). Sodium hydroxide, hydrochloric acid, ascorbic acid, gallic acid, aceticacid, methanol, $FeSO_4$, hydrogen peroxide, sodium salicylate, nutrient agar and tetracyclin were of analytical grade. They were obtained from Himedia (Mumbai, India). Double distilled water was used in all the experiments, with the exception of mosquitocidal ones. Tap water was used for the latter.

Collection and Processing of Crab Shells

Following the method by Murugan et al. [47], *X. testudinatus* hydrothermal vent crabs were collected from the North-East Taiwan coast, stored in Ziploc bags and refrigerated overnight. Using a meat tenderizer the exoskeletons of the crab were cut into smaller pieces. 20 g of crushed crab exoskeletons was measured using a Mettle balance, then labeled and oven-dried at 65 °C for four consecutive days to obtain constant weight. The dry weight of the samples was determined and the moisture content measured was based on the differences between the wet and the dry weight. The average moisture content of the crab exoskeletons was 15.66%.

Isolation and Extraction of Chitosan from Crab Shell

The chitosan recovering sequence involved washing of crushed crab exoskeletons in distilled water. Crushed crab exoskeletons were placed in 1000 mL beakers and soaked in boiling sodium hydroxide (2 and 4% w/v) for 1 h, in order to dissolve the proteins and sugars, thus isolating the crude chitin. 4% NaOH is used for chitin preparation, concentration used at the Sonat Corporation [35]. Then, the samples were boiled in the sodium hydroxide, the beakers containing the shell samples were removed from the hot plate, and allowed to cool for 30 min at room temperature [34]. The exoskeletons were then crushed to pieces of 0.5–5.0 mm using a meat tenderizer. The obtained pure chitosan was demineralized using 1% HCl (v: v) and 2% NaOH according to the method of Huang [27]. 50% NaOH was added to demineralized chitosan and boiled at 100 °C for 2 h on a hot plate then cooled for 30 min at room temperature. The process was repeated to deacetylate the chitosan powder and finally creamy-white form of chitosan was obtained [48].

Characterization of the Bio-Encapsulated Chitosan-Silver Nanocomplex

The AgNP were prepared by chemical reduction method, in which sodium citrate was used as reducing agent of $AgNO_3$. After the addition of trisodium citrate (1%

w/v) into $AgNO_3$ solution, the mixture was stirred for 2 h, then, treated with sonication at 1.5 kW for 30 min. The prepared silver solution was added into the chitosan solution (1% w/v in 1% acetic acid) and stirred for 12 h. The thick white nanocomposite gel was obtained after loading of Ag nanoparticles into chitosan solution. The suspension was subsequently centrifuged at 12,000×*g* for 10 min at 4 °C. A brown-yellow solution indicated the formation of chitosan-Ag nanoparticles, since aqueous silver ions were reduced by the chitosan powder and thus generating stable chitosan-Ag nanoparticles, then used for characterization and biological assays.

Chitosan Encapsulation

The preparation process was based on a previous method [74] with some modifications. Here, $CaCO_3$ microparticles with a monodisperse diameter were prepared as the template. To achieve this, 0.21 g Na_2CO_3 and 0.29 g $CaCl_2{\cdot}5H_2O$ were mixed in 20 mL deionized water under magnetic agitation with 0.29 g PSS as an additive. After 30 min, the $CaCO_3$ microparticles were collected by centrifuged at 5000 rpm for 10 min and washed in water three times. The adsorption of polyelectrolytes (2 mg/mL) onto the $CaCO_3$ microparticles was performed in 0.1 M Tris–HCl buffer (pH 7.0) for 15 min followed by three washes in water. The PAH layer was deposited by the addition of 15 mL of a 1 mg/mL aqueous PAH solution. The mixture was incubated for 15 min under gentle shaking and excess polyelectrolytes were removed by centrifugation at 5000 rpm for 10 min and washed in water three times. After assembly of the four subsequent polyelectrolyte bilayers of PSS/PAH/PSS/PAH, the particles were created by dissolving the $CaCO_3$ core in 0.2 M ethylene-di-amine-tetra-acetic acid solution (100 mM Tris–HCL buffer at pH 7) for 30 in under agitation and subsequently centrifuging the solution 5000 rpm for 10 min, after washing in water, the hollow microcapsules were re-dispersed in 10 mL of chitosan nanoparticle solution. The mixture was incubated at room temperature for 15 min. The chitosan-Ag nanoparticle loaded microcapsules were obtained after centrifugation at 5000 rpm for 10 min and the pellets were dried for the testing phase.

Characterization of Encapsulated Chitosan Silver Nanoparticles

The presence of bio-encapsulated chitosan-Ag nanocomplex was confirmed by sampling the reaction mixture at regular intervals, and the absorption maxima was scanned by UV–Vis, at the wavelength of 200–700 nm in a UV-3600 Shimadzu spectrophotometer at 1-nm resolution. Furthermore, the reaction mixture was subjected to centrifugation at 15,000 rpm for 20 min, and the resulting pellet was dissolved in deionized water and filtered through a Millipore filter (0.45 μm). The structure and composition of bio-encapsulated nanocomplex was analyzed by using a 10-kV ultrahigh-resolution scanning electron microscope (SEM); 25 μL of sample was sputter coated on a copper stub, and the morphology of the nanocomplex was investigated using a FEI QUANTA-200 SEM. Surface groups of chitosan-Ag nanocomplex were qualitatively confirmed by using FTIR spectroscopy [69], with

spectra recorded by a Perkin-Elmer Spectrum 2000 FTIR spectrophotometer. In addition, XRD and EDAX were also analyzed for the presence of metals in the sample [33, 47].

Free Radical Scavenging Potential

DPPH Scavenging Activity

The scavenging effect of chitosan-Ag nanoparticles and bio-encapsulated chitosan-Ag nanoparticles on DPPH radicals was determined to the method by [67]. Various concentrations of the sample (4 mL) were mixed with 1 mL of methanolic solution containing DPPH radicals, resulting in the final concentration of DPPH being 0.2 mM. The mixture was shaken vigorously and left to stand for 30 min, and the absorbance was measured at 517 nm. The percentage inhibition was calculated according to the formula: (0 - A1)/A0] $\times$ 100, where A0 was the absorbance of the control and A1 was the absorbance of the sample.

ABTS Radical Cation Scavenging Activity

The ABTS radical cation scavenging activity was performed as described by Re et al. [59], with slight modifications. $ABTS^{-+}$ cation radicals were produced by the reaction between 7 mM ABTS in water and 2.45 mM potassium persulfate, stored in the dark at room temperature for about 12 h. Prior to use, the solution was diluted with ethanol to get an absorbance at 734 nm. Free radical scavenging activity was assessed by mixing 10 µL of chitosan-Ag nanoparticles or bio-encapsulated chitosan-Ag nanoparticles with 1.0 mL of ABTS working standard in a micro-cuvette. The decrease in absorbance was measured exactly after 6 min. The percentage inhibition was calculated according to the formula: [(A0 - A1)/A0] $\times$ 100, where A0 was the absorbance of the control without the sample, and A1 was the absorbance of the sample.

Cytotoxicity on Breast Cancer Cells

Cell Lines

Human breast cancer cell line MCF 7 was purchased from National Centre for Cell Sciences (NCCS, Pune, India). Cells were maintained in DMEM with 10% fetal bovine serum, 1% penicillin and 0.5% streptomycin. The cultured cells were maintained at 37 °C in 5% CO_2 humidified incubator.

Cell Viability Assay

Cell proliferation was analyzed by 3-(4,5-dimethylthiazol-2-yl)- 2,5-di-phenyl-tetrazolium bromide (MTT) assay, as described by Mosmann [42]. Briefly, exponentially growing MCF-7 cells (1×10^4 cells per mL) were seeded in 96-well plates in a final volume of 100 mL per well and treated with series (1–50 mg/

mL) of the bio-encapsulated chitosan-Ag nanocomplex in FCS free complete medium for 48 h. 100 mL of MTT (5 mg/mL) was added to treated cells, and the plates were incubated at 37 °C for 4 h. The supernatant was aspirated and 100 mL of DMSO was added to each well to dissolve the formosan crystals. Absorbance was measured at 620 nm using a 96-well microplate reader (Lambda 1050 Perkin elmer) and the bio-encapsulated chitosan-Ag nanocomplex inhibitory concentrations (IC_{50}) causing the 50% reduction in cell viability was estimated. The percentage of cell survival was calculated using the following formula [41].

$$\text{Relative cell survival } (\%) = (\text{Mean experimental cell absorbance (A620)}/ (\text{Mean control cell absorbance (A620)}) \times 100$$

Apoptosis

Flow cytometry was used to detect apoptotic cells with diminished DNA content. MCF-7 cells were seeded into 6-well plates at 1×10^5 cells/well. Post-treatment with the bio-encapsulated chitosan-Ag nanocomplex, cells were fixed in ice-cold 70% ethanol at −20 °C overnight. After centrifugation and washing one time with PBS, low-molecular-weight DNA was extracted using 0.2 mol/l phosphate–citrate buffer and stained with 200 µL of 1 mg/mL propidium iodine (PI)/10 mL, and 0.1% Triton X-100/2 mg DNase-free RNase A. The solution was then incubated for 30 min at room temperature in the dark, followed by flow cytometric analysis at 488 nm (BD, Franklin Lakes, NJ, USA).

Toxicity Against Malaria Mosquitoes

Mosquito Rearing

Eggs of *A. stephensi* were provided by the National Centre for Disease Control (NCDC) field station of Mettupalayam (Tamil Nadu, India). Eggs were transferred to laboratory conditions [27 ± 2 °C, 75–85% R.H., 14:10 (L:D) photoperiod] and placed in $18 \times 13 \times 4$ cm^3 plastic containers containing 500 mL of tap water, to await larval hatching [16, 72]. Larvae were reared in these containers and fed daily with a mixture of crushed dog biscuits (Pedigree, USA) and hydrolyzed yeast (Sigma-Aldrich, Germany) at a 3:1 ratio (w:w). Water was renewed every 2 days. The breeding medium was checked daily and dead individuals were removed. Breeding containers were kept closed with muslin cloth to prevent contamination by foreign mosquitoes. Pupae were collected daily from culture containers and transferred to glass beakers containing 500 mL of water. Each glass beaker contained about 50 mosquito pupae and was placed in a mosquito-rearing cage ($90 \times 90 \times 90$ cm^3, plastic frames with chiffon walls) until adult emergence. Mosquito adults were continuously provided with 10% (w:v) glucose solution on cotton wicks. The cotton was always kept moist with the solution and changed daily. Five days after emergence, females were sup- plied with a blood meal which was furnished by means of professional heating blood (lamb blood), at a fixed

temperature of 38 °C and enclosed in a membrane of cow gut. After 30 min, the blood meal was removed and a fresh one was introduced [45, 46].

Laboratory Conditions

The mosquitocidal activity of bio-encapsulated chitosan-Ag nanocomplex against *A. stephensi* was assessed as described by Murugan et al. [47], 25 *A. stephensi* larvae (I, II, III, or IV instar) or pupae were placed in 500-mL beakers and exposed for 24 h to dosages of 25, 50, 75, 100 and 125 ppm (bio-encapsulated chitosan-Ag nanocomplex) and 5, 10, 15, 20 and 25 ppm (chitosan-Ag nanocomplex). A 0.5-mg larval food was provided for each test concentration. For each experiment, three replicates were maintained at a time. Percentage mortality was calculated as follows:

$$\text{Mortality } (\%) = (\text{Number of dead individuals}/\text{Number of treated individuals}) \times 100$$

Field Assays

The mosquitocidal activity of the chitosan-Ag nanocomplex and bio-encapsulated chitosan-Ag nanocomplex on *A. stephensi* was evaluated in field conditions, testing them in six external water reservoirs at the NCDC (Coimbatore, India), using a knapsack sprayer (Private Limited 2008, Ignition Products, India). Pre-treatment and post-treatment (at 24, 48, 72, and 96 h) larval density was monitored using a larval dipper [16]. Toxicity was assessed against third- and fourth instar larvae. Larvae were counted and identified to specific level. More than 92% of all surveyed larvae belong to *An. stephensi*. Six trials were conducted for each test site with similar weather conditions (27 ± 2 °C; 79% R.H.). The required quantity of mosquitocidal was calculated on the basis of the total surface area and volume (0.25 m^3 and 250 L); the required concentration was prepared using 10× the observed laboratory LC_{50} values [72]. Percentage reduction of the larval density was calculated using the formula:

$$\text{Percentage reduction} = (C - T)/C \times 100$$

where C is the control and T is treatment.

Impact on Larvivorous Fish Predation

First, the predation efficiency of *P. reticulata* fishes was assessed *A. stephensi* larvae in standard laboratory conditions. For each instar, 500 mosquitoes were introduced, with one fish, in a 500-mL glass beaker containing 250 mL of dechlorinated water. Mosquito larvae were replaced daily with new ones. For each mosquito instar, four replicates were conducted. Control was 250 mL of dechlorinated water without fishes. All beakers were checked after 1, 2, 3, 4, and 5 days and the number of prey consumed by fishes was recorded. The predatory efficiency was calculated using the

following formula: Predatory efficiency = (Number of consumed mosquitoes/Number of predators) $TotalNumberofmosquitoes \times 100$. In the second experiment, the predation efficiency of *P. reticulata* was assessed against *A. stephensi* larvae, after a mosquitocidal treatment with bio-encapsulated chitosan-Ag nanocomplex. For each instar, 500 mosquitoes were introduced with one fish in a 500-mL glass beaker filled with 249 mL of dechlorinated water and 1 mL of the desired concentration of the bio-encapsulated chitosan-Ag nanocomplex (1/3 of the LC_{50} calculated on first instar larvae). Mosquito larvae were replaced daily with new ones. For each mosquito instar, four replicates were conducted. Control was 250 mL of water. All beakers were checked after 1, 2, 3, 4, and 5 days and the number of prey consumed by fishes was recorded. Predatory efficiency was calculated using the above-mentioned formula.

Data Analysis

SPSS version 16.0 was used for the analyses. Larvicidal and pupicidal data were subjected to probit analysis. LC_{50} and LC_{90} were calculated using the method by Finney [17]. Antioxidant and anticancer data were analyzed using ANOVA followed by Tukey's HSD test ($P = 0.05$). Fish predation data were analyzed by JMP 7 using a weighted general linear model with two fixed factor: $y = X\beta + \varepsilon$ where y is the vector of the observations (i.e. the number of consumed preys), X is the incidence matrix, ß is the vector of fixed effect (i.e. the treatment and the targeted mosquito instar), and ε is the vector of the random residual effects. A probability level of $P < 0.05$ was used for the significance of differences between values.

Results and Discussion

Fabrication and Characterization of the Bio-Encapsulated Chitosan-Ag Nanocomplex

The synthesis of nanoparticle was initiated once the chitosan powder was introduced into aqueous $AgNO_3$. AgNP exhibited dark brown color after 4 h. The formation and stability of AgNP in aqueous solution of chitosan powder was confirmed by using UV–Vis spectroscopy at 448–440 nm. The color change occurred because the active molecules present in the extract reduced silver ions into AgNPs. The bio-encapsulated chitosan-Ag nanocomplex exhibited a strong peak at 441 nm (Fig. 1a), which may be due to excitation of surface Plasmon vibrations in chitosan-Ag nanocpmplex [9, 50].

The FTIR spectrum of bio-encapsulated chitosan-Ag nanocomplex showed transmittance peaks at amines group region (Fig. 1b). The stretching frequencies were observed at 3744, 3341, 2489, 2438, 1876, 1644, 1072, 996, 843 and 789 cm^{-1}. The O–H and N–H stretching frequency exhibited a band at 3341 cm^{-1}. The band at 2489 cm^{-1} may correspond to alkanyl C=C stretch. Bio-encapsulated chitosan-Ag nanocomplex acquired a small vibration band at 1876 cm^{-1} probably corresponding to stretching proteins bonds. The carbonyl stretching absorption is one of the strongest

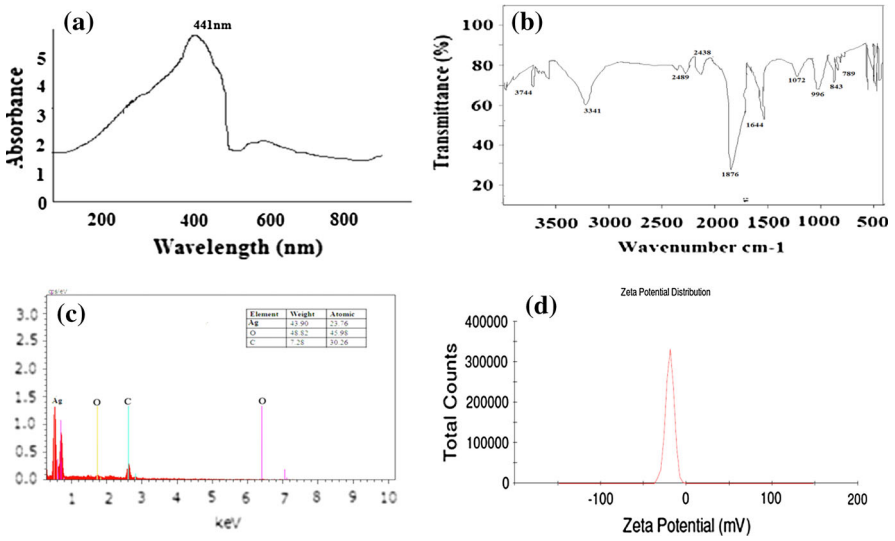

Fig. 1 Biophysical characterization of bio-encapsulated chitosan-silver nanocomplex: **a** UV–Vis spectrum, **b** functional group prediction by FTIR spectroscopy, **c** EDAX pattern, and **d** Zeta potential analysis

IR absorptions, and is very useful in structure determination as one can determine both the number of carbonyl groups but also an estimation of which types. The band at 1072 cm^{-1} shows the skeletal vibrations involving O–C stretching frequency. The peak at 996 cm^{-1} could be allotted to the ether linkages or –C–O–C– stretch. The peaks at 789 cm^{-1} are aromatic C–H bending in bio-encapsulated chitosan-Ag nanocomplex. These stretching and bending frequencies peaks might be due to the stretching between the carbon and hydrogen bonds present in chitosan. These peaks could also indicate that a carbonyl group formed amino acid residues and that these residues capped AgNP to prevent agglomeration, thus stabilizing the medium [63]. Overall, our results suggest that molecules capping chitosan-Ag nanoparticles had free and bound amide groups. These amide groups may also be linked to the aromatic rings. We hypothesize that these compounds may belong to polyphenols with an aromatic ring and bound amide region [31, 32].

SEM of the chitosan-Ag nanocomplex was recorded at high magnifications, their morphology showed predominantly spherical and cubic structures with a size range of 100 nm (Fig. 2). The capsule-like cubic shape in Fig. 2 highlighted the capsule formation. The spherical and cubic structure of chitosan indicates the formation of proper encapsulation around the nanocomplex. SEM elucidated the bio-reducing potency of chitosan, which mediated the biosynthesis of AgNP [52]. Standard energy-dispersive X-ray (EDX) spectrum recorded on the examined SEM samples showed strong energy peaks for Ag in the range of Ag characteristic lines K and L was given in Fig. 1c. The result coincides with the EDX pattern of *Kedrostis foeditissima*-mediated Ag nanoparticles [49].

It should be noted that the nanoparticles with Zeta potential values higher than +30 mV or lower than −30 mV are considered stable [50]. Zeta potential value of

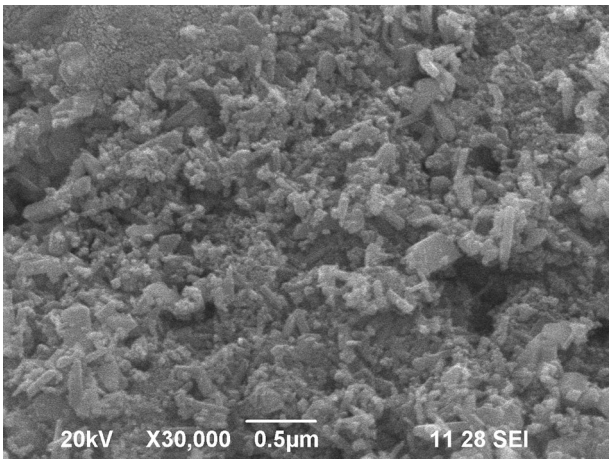

Fig. 2 FESEM of bio-encapsulated chitosan-silver nanocomplex

the bio-encapsulated chitosan-Ag nanocomplex was −19.3 mV (Fig. 1d), confirming the high stability of the nanocomplex tested in this research.

Free Radical (DPPH and ABTs) Scavenging Activity

DPPH and ABTS radical scavenging methods are common spectrophotometric procedures for determining antioxidant capacities of components, and they are based on the ability of ABTS and DPPH radical to decolorize in the presence of antioxidants by accepting an electron or hydrogen donated by an antioxidant compound [37]. The DPPH and ABTs scavenging potential of bio-encapsulated chitosan-Ag nanocomplex and non-encapsulated nano-products at different concentrations was given in Fig. 3. The assay based on the measurement of scavenging ability of chitosan-Ag nanocomplex and bio-encapsulated chitosan-Ag nanocomplex towards stable DPPH radical and a mono cation ABTs. Whose quenching ability increased with increasing concentration of 0.2–1 mg/mL in dose-dependent manner. In radical form, DPPH absorbs at 517 nm, but upon reduction with an antioxidant, its absorption decreases due to the formation of its non-radical form, DPPH–H. Bio-encapsulated chitosan-Ag nanocomplex highly scavenges DPPH (Fig. 3a) and ABTS (Fig. 3b) when compared to the chitosan-Ag nanocomplex alone. It has been reported that chitosan scavenges various free radicals through the action of nitrogen on the C-2 position of the chitosan [58]. The nitrogen of amino groups has a lone pair of electrons; it can attach to a proton released from acidic solution to form ammonium (NH_3^+) groups. The free radicals can react with the hydrogen ion from the NH_3^+ to form a stable molecule. Thus, here the bio-encapsulated chitosan-Ag nanocomplex acted as hydrogen donating antioxidant in order to decrease the absorbance of DPPH solution, this was in agreement with the findings by Jaganathan et al. [33] and Murugan et al. [47]. Therefore, the DPPH and ABTS radical scavenging activity of bio-encapsulated chitosan-Ag nanocomplex

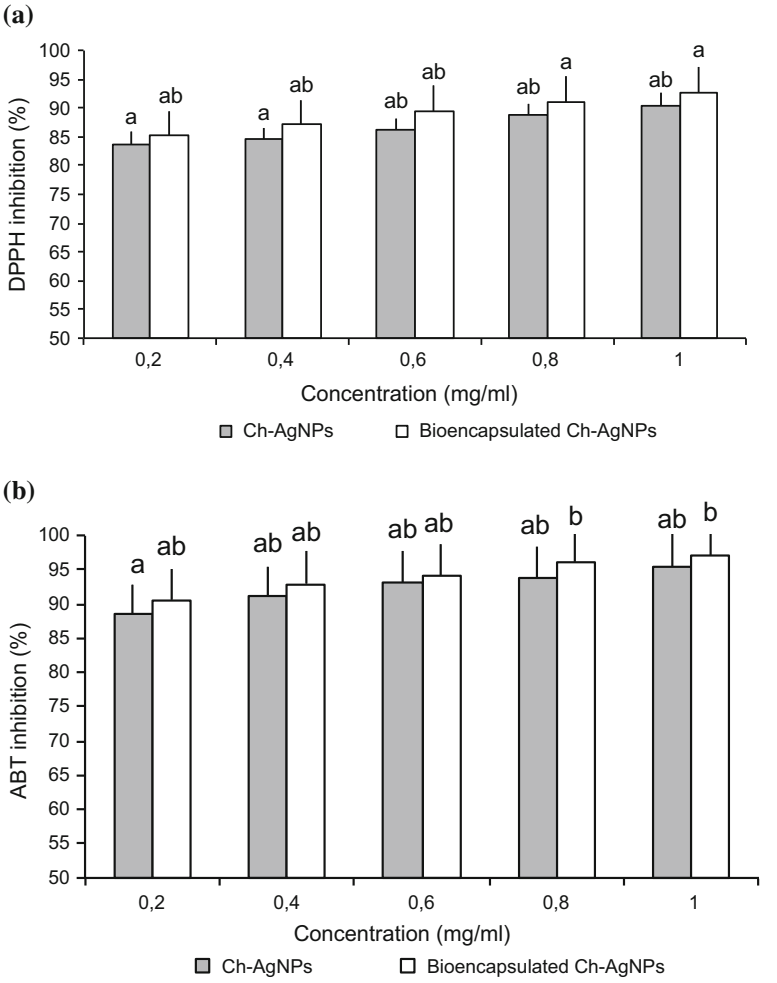

Fig. 3 Free radical scavenging potential of chitosan-fabricated silver nanoparticles and bio-encapsulated chitosan-silver nanocomplex: **a** DPPH and **b** ABTS scavenging effect. *T-bars* represent standard deviations. Above each column, *different letters* indicate significant differences (P = 0.05). Ch-AgNPs = chitosan-silver nanocomplex

was effective than chitosan and AgNps alone indicating its ability to scavenge free radicals, thereby preventing lipid oxidation via radical scavenging or a chain-breaking reaction.

Cytotoxicity and Apoptosis-Triggering Pathways on Human Breast Cancer Cells

Following the results of free radical scavenging assays, the bio-encapsulated chitosan-Ag nanocomplex was selected for in vitro cytotoxicity on breast carcinoma cells (MCF-7) using MTT assay. MCF-7 cells were treated with increasing

concentration (1.88, 3.75, 7.5, 1.5 and 30 µg/mL) of bio-encapsulated chitosan-Ag nanocomplex which exerted a decrease in cell viability. IC_{50} was 17.79 µg/mL at 48 h exposure, with $R^2 = 0.974$ (Fig. 4). The reduced cell viability induced by exposure to bio-encapsulated chitosan-Ag nanocomplex was achieved by the production the reactive ROS causing a damage to cellular components leading to intracellular oxidative stress, ending up in apoptosis and necrosis (Fig. 4). Gnanadhas et al. [19] also demonstrated that the potential of AgNPs was based on the type of capping agent used. Several other studies also reported that capping agents stabilized the AgNPs by decreasing aggregation of the particles and providing protection from temperature and light [2, 28]. Notably, enhanced toxicity was observed when AgNPs were coated with different capping agents. For examples, Murdock et al. [43] found that the addition of serum to cell culture media had a significant effect on particle toxicity, possibly due to changes in agglomeration or surface chemistry. Also, chitosan-pluronic polymeric nanoparticles were used against breast cancer cells [1, 61]. From our results, we argued that the bio-encapsulated chitosan-Ag nanocomplex is a potential candidate in inhibiting tumor progression with little toxicity to normal cells [47].

The flow cytometer analysis at 488 nm quantified the production of apoptotic cells, monitoring reduced DNA content; 1–6.1% was the apoptotic cell percentage revealed by the effect of bio-encapsulated chitosan-Ag nanocomplex against MCF-7 cells, apoptosis increased significantly with the tested dose, $R^2 = 0.965$ (Fig. 4). Overall, the bio-encapsulated chitosan-Ag nanocomplex is a promising candidate to initiate Bax/Bcl-2/cytochrome c/caspase-3 signaling pathway for enhancing the apoptosis of MCF-7 cells [33].

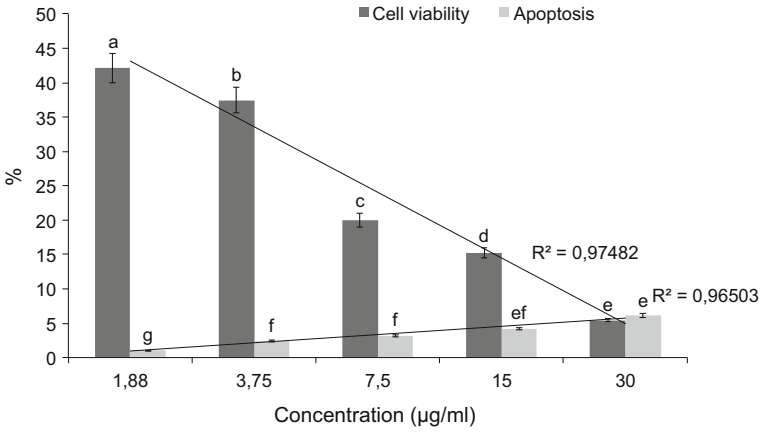

Fig. 4 Cytotoxicity (%) and triggered apoptosis (%) on MCF-7 cells post-treatment with the bio-encapsulated chitosan-silver nanocomplex. *T-bars* represent standard deviations. Above each column, *different letters* indicate significant differences ($P = 0.05$)

Larvicidal and Pupicidal Activity

In laboratory conditions, the chitosan-Ag nanocomplex and the bio-encapsulated chitosan-Ag nanocomplex were tested for their toxicity on larvae and pupae of *A. stephensi*. The bio-encapsulated chitosan-Ag nanocomplex exhibited LC_{50} values of 54.652 ppm (larva I), 62.380 ppm (II), 73.236 ppm (III), 85.291 ppm (IV) and 98.172 ppm (pupa) (Table 1), while chitosan-Ag nanocomplex achieved lower LC_{50}, i.e. 4.432 ppm (larvaI), 4.975 ppm (II), 5.543 ppm (III), 6.511 ppm (IV) and 7.641 ppm (pupa) (Table 2). The higher toxicity of chitosan-Ag nanocomplex, which is in agreement with [47], may be due to the slower release of nanoparticles in the bio-encapsulated chitosan-Ag nanocomplex treatment. However, this may also represent an advantage, allowing long-term release of stable mosquitocides in the aquatic environment (see also [3]), while *A. aegypti* was controlled using chitosan nanoparticles on third instar larvae [62]; larval mortality, growth inhibition and antifeedant activity evoked by chitosan compounds were also reported on third instar larvae of *Spodoptera littoralis* (Badawy and Aswad [4]).

Table 1 Acute toxicity of the bio-encapsulated chitosan-silver nanocomposite on larvae of the malaria vector *Anopheles stephensi*

Target	LC_{50} (LC_{90})	95% Confidence limit		Regression equation	X^2 (d.f. = 3)
		LC_{50}(LC_{90})			
		LCL	UCL		
Larva I	54.652 (106.887)	49.538 (98.003)	59.541 (119.243)	$y = 1.341 + 0.025x$	4.068 n.s
Larva II	62.380 (124.120)	56.704 (111.979)	68.243 (142.047)	$y = 1.295 + 0.021x$	1.962 n.s
Larva III	73.236 (140.044)	67.057 (124.813)	80.549 (163.471)	$y = 1405 + 0.019x$	1.264 n.s
Larva IV	85.291 (156.637)	77.910 (137.649)	95.292 (187.208)	$y = 1.532 + 0.018x$	1.246 n.s
Pupa	98.172 (175.534)	88.575 (151.233)	112.904 (217.255)	$y = 1.626 + 0.017x$	0.175 n.s

No mortality was observed in the control

LC_{50} lethal concentration that kills 50% of the exposed organisms

LC_{90} lethal concentration that kills 90% of the exposed organisms

LCL lower confidence limit

UCL upper confidence limit

χ^2 Chi square value

d.f. degrees of freedom

n.s. not significant (P = 0.05)

Table 2 Acute toxicity of the chitosan-fabricated silver nanoparticles on the malaria vector *Anopheles stephensi*

Target	LC_{50} (LC_{90})	95% Confidence Limit		Regression equation	X^2
		LC_{50}(LC_{90})			
		LCL	UCL		
Larva I	4.432 (9.398)	0.089 (7.110)	6.498 (21.511)	$y = 1.144 + 0.0258x$	17.930 n.s
Larva II	4.975 (10.556)	2.424 (8.271)	6.727 (18.762)	$y = 1.142 + 0.230x$	11.101 n.s
Larva III	5.543 (11.888)	4.934 (10.704)	6.123 (13.648)	$y = 1.120 + 0.202x$	4.925 n.s
Larva IV	6.511 (13.092)	5.914 (11.719)	7.152 (15.171)	$y = 1.268 + 0.195x$	4.179 n.s
Pupa	7.641 (14.703)	6.977 (12.998)	8.463 (17.395)	$y = 1.386 + 0.181x$	2.506 n.s

No mortality was observed in the control

LC_{50} lethal concentration that kills 50% of the exposed organisms

LC_{90} lethal concentration that kills 90% of the exposed organisms

LCL lower confidence limit

UCL upper confidence limit

χ^2 Chi square value

d.f. degrees of freedom

n.s. not significant (P = 0.05)

Larvicidal Toxicity in the Field

A field trial was conducted evaluating the bio-encapsulated chitosan-Ag nanocomplex against malaria mosquitoes (Table 3). The application of bio-encapsulated chitosan-Ag nanocomplex led to the reduced larval populations of *A. stephensi* by 86.2, 48.4 and 100% after the exposure period of 24, 48 and 72 h, respectively

Table 3 Field effectiveness of bio-encapsulated chitosan-Ag nanocomposite and chitosan-fabricated Ag nanoparticles against larvae of the malaria vector *Anopheles stephensi*

Treatment	Larval density (n)			
	Before treatment	24 h	48 h	72 h
Bio-encapsulated chitosan-silver nanocomposite (10 × LD_{50})	127.4 ± 14.79[a]	86.2 ± 15.07[b]	48.4 ± 7.43[c]	0.0 ± 0.0[d]
Chitosan-fabricated silver nanoparticles (10 × LD_{50})	107.4 ± 12.79[a]	68.8 ± 13.40[b]	36.4 ± 7.89[c]	0.0 ± 0.0[d]

Larval densities are expressed as mean ± SD of five replicates

Nomortality was observed in the control

Within each row, means followed by the same letter(s) are not significantly different (ANOVA, Tukey's HSD test, P = 0.05)

(Table 3). Comparably, the 10 × LC_{50} values of chitosan-Ag nanocomplex led to 68.8, 36.4 and 100% reduction of *A. stephensi.* The efficiency of bio-encapsulated chitosan-Ag nanocomplex was comparable with neem-based treatments, which delayed phenology of surviving larvae and reduced pupal weight [80, 81]. Moreover, in field studies Bti (*Bacillus thuringiensis* var. *israelensis*) has been shown as effective on several mosquito species in widely differing water quality conditions, including irrigated pastures, storm drains, ponds, dairy lagoons, and salt marsh potholes [51]. Recently, *A. aegypti* larval reduction of 47.6, 76.7, and 100%, while the *Phyllanthus niruri* extract led to 39.9, 69.2, and 100% of larval reduction after 24, 48, and 72 h, respectively [72]. Also, the mosquitocidal efficacy of the leaf extract of *Euphorbia hirta* was investigated in the field condition on *A. stephensi*, and larval density was reduced by 13.17, 37.64 and 84.00% after 24, 48, and 72 h, respectively [54], but see also [65].

Impact on Longevity and Fecundity of Malaria Mosquitoes

Male and female *Anopheles stephensi* was studied for longevity and fecundity post-treatment with the chitosan-Ag nanocomplex and the bio-encapsulated chitosan-Ag nanocomplex. The treatment with chitosan-Ag nanocomplex at 3.125, 6.25, 12.5, 25 and 50 ppm reduced longevity as follows: 15.2, 13.4, 11.2, 8.6, 6.2 days (males) and 31.4, 27.4, 24.2, 19.2, 15.6 days (females) in a dose-dependent manner (Table 4). Testing bio-encapsulated chitosan-Ag nanocomplex, the highly reduced adult longevity was found to be 12.4, 10.4, 8.2, 6.4, 5.0 (male) and 26.4, 24.0, 17.6, 15.4, 12.8 (female) whose control had 12.4 days (male) and 26.4 days (female) (Table 5).

The number of eggs laid was inversely proportional to the concentration of chitosan-Ag nanocomplex used in the treatment. The egg hatchability was reduced (fecundity) to 135.2, 120.2, 113.2, 85.6 and 70.4 eggs (Table 5), comparatively 140.4 eggs were recorded when testing the chitosan-Ag nanocomplex. In bio-

Table 4 Impact of chitosan-fabricated silver nanoparticles on longevity and fecundity of *Anopheles stephensi* adults

Treatment (ppm)	Adult longevity (days)		Fecundity (no. of eggs)
	Male	Female	
Control	18.4 ± 1.94^{e}	34.2 ± 1.64^{e}	140.4 ± 1.81^{d}
3.125	15.2 ± 1.78^{de}	31.4 ± 2.50^{de}	135.2 ± 2.38^{d}
6.25	13.4 ± 2.40^{cd}	27.4 ± 2.50^{cd}	120.2 ± 2.86^{c}
12.5	11.2 ± 1.48^{bc}	24.2 ± 1.92^{bc}	113.2 ± 2.28^{c}
25	8.6 ± 2.07^{ab}	19.2 ± 2.86^{ab}	85.6 ± 2.40^{b}
50	6.2 ± 1.92^{a}	15.6 ± 2.07^{a}	70.4 ± 1.67^{a}

Within each column, means followed by the same letter(s) are not significantly different (ANOVA, Tukey's HSD test, P = 0.05)

Table 5 Impact of bio-encapsulated chitosan-fabricated silver nanoparticles on longevity and fecundity of *Anopheles stephensi* adults

Treatment (ppm)	Adult longevity (days)		Fecundity (no. of eggs)
	Male	Female	
Control	18.4 ± 1.94^{e}	34.2 ± 1.64^{e}	140.4 ± 1.81^{f}
3.125	12.4 ± 1.81^{d}	26.4 ± 1.81^{d}	130.8 ± 3.19^{e}
6.25	10.4 ± 1.67^{cd}	24.0 ± 2.00^{c}	114.4 ± 2.40^{d}
12.5	8.2 ± 0.83^{bc}	17.6 ± 1.51^{b}	109.4 ± 1.81^{c}
25	6.4 ± 1.14^{ab}	15.4 ± 1.51^{ab}	75.6 ± 2.07^{b}
50	5.0 ± 1.22^{a}	12.8 ± 1.78^{a}	64.4 ± 1.67^{a}

Within each column, means followed by the same letter(s) are not significantly different (ANOVA, Tukey's HSD test, $P = 0.05$)

encapsulated chitosan-Ag nanocomplex experiment, 137.4 eggs were recorded in control and the number of eggs recorded in the treatment was 130.8, 114.4, 109.4, 75.6, and 64.4 eggs (Table 5). Recently the impact on larvicidal toxicity, fecundity and longevity of *A. stephensi* on *Bacillus sphaericus* has been investigated by [31, 32], while the interactive effect of botanicals (neem, *Pongamia* and *Leucas aspera*) and *Bacillus sphericus* against the larvae of *Culex quinquefasciatus* has been studied by Murugan et al. [44]. Furthermore, comparable effects have been reported on mosquito populations treated with microbial insecticides. For instance, reductions of longevity and fecundity have been reported on *A. stephensi* and *C. quinquefasciatus* treated with *Bacillus sphaericus* (GR strain) [31, 32, 39, 70].

Predation of *P. reticulata* Post-Treatment with the Bioencapsulated Chitosan-Silver Nanocomplex

In laboratory conditions, the larvivorous fish *P. reticulata* showed effective predation against *A. stephensi* within 24 h. Predatory efficiency towards II and III instar larvae of *A. stephensi* were 70.25% (II) and 46.75% (III). In our observations, III instar larvae were preferred by *P. reticulata*. This may be linked to the size of these mosquito predators, which are advantaged by predating on bigger and slower preys [7]. Interestingly, the predatory efficiency of *P. reticulata* was not reduced by a previous treatment with bio-encapsulated chitosan-Ag nanocomplex. After 24 h, the predatory efficacy of *P. reticulata* after treatment was 88.50% against II instar larvae and 70.25% against III instar larvae (Fig. 5). Similarly, it has been demonstrated that the predation rates of *Danio rerio* fishes post-treatment with chitosan-synthesized AgNP were higher, 89.5, 77.3, 68.3 and 61.5 larvae (I, II, III and IV, respectively) over standard conditions [47]. Notably, recent researches showed that the green-synthesized mosquitocidal AgNP showed, as a general trend, extremely low toxicity rates against non-target organisms, such as predators of mosquito young instars (e.g. [21–25]).

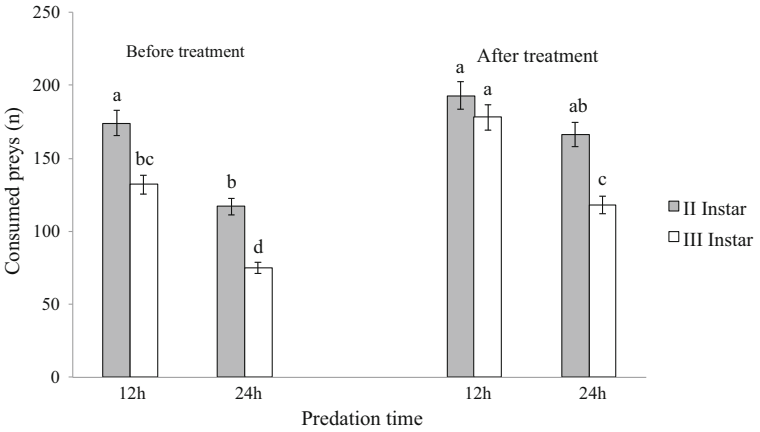

Fig. 5 Predation efficiency of the larvivorous fish *Poecilia reticulata* against larvae of the malaria vector *Anopheles stephensi* before and post-treatment with the bioencapsulated chitosan-silver nanocomplex. *T-bars* represent standard deviations. Above each column, *different letters* indicate significant differences ($P = 0.05$)

Conclusions

Overall, in this study, we cheaply and quickly fabricated a bioencapsulated chitosan-silver nanocomplex, which was characterized by UV–Vis spectroscopy, FTIR, EDX, SEM, XRD and Zeta potential analyses. The nanocomplex was efficient as scavenger of free radicals (DPPH and ABTS), if compared to non-encapsulated chitosan-Ag nanocomplex. In toxicity assays against breast cancer cells (MCF-7) the bio-encapsulated chitosan-Ag nanocomplex triggered apoptotic pathways, leading to a rapid decline of MCF-7 cell viability. Furthermore, the bio-encapsulated chitosan-Ag nanocomplex was effective against *A. stephensi* both in laboratory and in the field. Notably, the bio-encapsulated chitosan-Ag nanocomplex also reduced longevity and fecundity of *A. stephensi*, and did not showed detrimental effects on predation rates of *P. reticulata* fishes on mosquito larvae, thus it can be considered further for the development of stable and long-term effective mosquitocidal formulations.

Acknowledgements Dr. Anitha Jaganathan is grateful to the University Grant Commission, New Delhi, India, Project No. PDFSS-2014-15-SC-TAM-10125.

References

1. M. Almada, M. G. Burboa, E. Robles, L. E. Gutierrez, M. A. Valdes, and J. Juarez (2014). Interaction and cytotoxic effects of hydrophobized chitosan nanoparticles on MDA-MB-231, HeLa and Arpe-19 cell lines. *Curr. Top. Med. Chem.* **14**, (6), 692–701.
2. E. Amato, Y. A. Diaz-Fernandez, A. Taglietti, P. Pallavicini, L. Pasotti, L. Cucca, C. Milanese, P. Grisoli, C. Dacarro, J. M. Fernandez-Hechavarria, and V. Necchi (2011). Synthesis, characterization and antibacterial activity against gram positive and gram negative bacteria of biomimetically coated silver nanoparticles. *Langmuir* **27**, (15), 9165–9173.

3. M. Anand, R. Kalaivani, M. Maruthupandy, A. K. Kumaraguru, and S. Suresh (2014). Extraction and characterization of chitosan from marine crab and squilla collected from the Gulf of Mannar Region. *J. Chitin Chitosan Sci.* **2**, 1.
4. M. E. I. Badawy and A. F. EL-Aswad (2012). Insecticidal activity of chitosans of different molecular weights and chitosan-metal complexes against cotton leaf worm *Spodoptera littoralis* and oleander aphid *Aphis nerii*. *Plant Protect. Sci.* **48**, (3), 131–141.
5. G. Benelli (2015). Research in mosquito control: current challenges for a brighter future. *Parasitol. Res.* **114**, 2801–2805.
6. G. Benelli (2015). Plant-borne ovicides in the fight against mosquito vectors of medical and veterinary importance: a systematic review. *Parasitol. Res.* **114**, 3201–3212.
7. G. Benelli (2016). Plant-mediated biosynthesis of nanoparticles as an emerging tool against mosquitoes of medical and veterinary importance: a review. *Parasitol. Res.* **115**, 23–34.
8. G. Benelli (2016). Plant-mediated synthesis of nanoparticles: anewer and safer tool against mosquito-borne diseases? *Asia Pacif. J. Trop. Biomed.* doi:10.1016/j.apjtb.2015.10.015.
9. G. Benelli (2016). Green synthesized nanoparticles in the fight against mosquito-borne diseases and cancer—a brief review. *Enzym. Microb. Technol.* doi:10.1016/j.enzmictec.2016.08.022.
10. G. Benelli and H. Mehlhorn (2016). Declining malaria, rising dengue and Zika virus: insights for mosquito vector control. *Parasitol. Res.* doi:10.1007/s00436-016-4971-z.
11. G. Benelli, R. Pavela, A. Canale, and H. Mehlhorn (2016). Tick repellents and acaricides of botanical origin: a green roadmap to control tick-borne diseases? *Parasitol. Res.* doi:10.1007/s00436-016-5095-1.
12. G. Benelli, A. Lo Iacono, A. Canale, and H. Mehlhorn (2016). Mosquito vectors and the spread of cancer: an overlooked connection? *Parasitol. Res.* **115**, 2131–2137. doi:10.1007/s00436-016-5037-y.
13. G. Benelli, A. Canale, A. Higuchi, K. Murugan, R. Pavela, and M. Nicoletti (2016). The outbreaks of Zika virus: mosquito control faces a further challenge. *Asia Pacif. J. Trop. Dis.* **6**, 253–258.
14. M. Bittelli, M. Flury, G. S. Campbell, and E. J. Nichols (2001). Reduction of transpiration through foliar application of chitosan. *Agric. Meteorol.* **107**, 167–175.
15. T. B. Cahu, S. D. Santos, and A. Mendes (2012). Recovery of protein, chitin, carotenoids and glycosaminoglycans from Pacific white shrimp (*Litopenaeus vannamei*) processing waste. *Proc. Biochem.* **47**, (4), 570–577.
16. D. Dinesh, K. Murugan, P. Madhiyazhagan, C. Panneerselvam, M. Nicoletti, W. Jiang, G. Benelli, B. Chandramohan, and U. Suresh (2015). Mosquitocidal and antibacterial activity of green-synthesized silver nanoparticles from *Aloe vera* extracts: towards an effective tool against the malaria vector *Anopheles stephensi*? *Parasitol. Res.* **114**, 1519–1529.
17. D. J. Finney *Probit analysis*, 3rd ed (Cambridge University Press, Cambridge, 1971).
18. A. K. Gaharwar, N. A. Peppas, and A. Khademhosseini (2014). Nanocomposite hydrogels for biomedical applications. *Biotechnol. Bioeng.* **111**, (3), 441–453. doi:10.1002/bit.25160.
19. D. P. Gnanadhas, M. Ben Thomas, R. Thomas, A. M. Raichur, and D. Chakravortty (2013). Interaction of silver nanoparticles with serum proteins affects their antimicrobial activity in vivo. *Antimicrob. Agents Chemother.* **57**, (10), 4945–4955.
20. D. A. Gorin, D. G. Shchukin, A. I. Mikhailov, K. Kohler, S. A. Sergeev, S. A. Portnov, I. V. Taranov, V. V. Kislov, and G. B. Sukhorukov (2006). Effect of microwave radiation on polymer microcapsules containing inorganic nanoparticles. *Tech. Phys. Lett.* **32**, (1), 70–72.
21. M. Govindarajan and G. Benelli (2016). One-pot fabrication of silver nanocrystals using *Ormocarpum cochinchinense*: biophysical characterization of a potent mosquitocidal and biotoxicity on non-target mosquito predators. *J. Asia-Pacif. Entomol.* **19**, 377–385.
22. M. Govindarajan and G. Benelli (2016). Facile biosynthesis of silver nanoparticles using *Barleria cristata*: mosquitocidal potential and biotoxicity on three non-target aquatic organisms. *Parasitol. Res.* **115**, 925–935.
23. M. Govindarajan, S. L. Hoti, and G. Benelli (2016). Facile fabrication of eco-friendly nanomosquitocides: biophysical characterization and effectiveness on neglected tropical mosquito vectors. *Enzym. Microb. Technol.* doi:10.1016/j.enzmictec.2016.05.005.
24. M. Govindarajan, S. L. Hoti, M. Rajeswary, and G. Benelli (2016). One-step synthesis of polydispersed silver nanocrystals using *Malva sylvestris*: an eco-friendly mosquito larvicide with negligible impact on non-target aquatic organisms. *Parasitol. Res.* doi:10.1007/s00436-016-5038-x.
25. M. Govindarajan, M. Nicoletti, and G. Benelli (2016). Bio-physical characterization of polydispersed silver nanocrystals fabricated using *Carissa spinarum*: a potent tool against mosquito vectors. *J. Clust. Sci.* doi:10.1007/s10876-016-0977-z.

26. U. Hafeli, W. Schutt, J. Teller, and M. Zborowski *Scientific and clinical applications of magnetic carriers* (Plenum materials, New York, 1997).
27. M. Huang (2004). Uptake and cytotoxicity of chitosan molecules and nanoparticles: effects of molecular weight and degree of deacetylation. *Pharm. Res.* **21**, (2), 344–353.
28. S. Jaiswal, B. Duffy, A. K. Jaiswal, N. Stobie, and P. McHale (2010). Enhancement of the antibacterial properties of silver nanoparticles using beta-cyclodextrin as a capping agent. *Int. J. Antimicrobial. Agents* **36**, (3), 280–283.
29. K. Karunamoorthi (2012). Global malaria eradication: is it still achievable and practicable? *J. Malar. Res.* **2**, (1), 37–62.
30. C. Krishnaraj, E. G. Jagan, S. Rajasekar, P. Selvakumar, and P. T. Kalaichelvan (2010). Synthesis of silver nanoparticles using *Acalypha indica* leaf extracts and its antibacterial activity against water borne pathogens. *Colloids Surf. B* **76**, 50–56.
31. A. N. Kumar, K. Murugan, K. Shobana, and D. Abirami (2013). Isolation of *Bacillus sphaericus* screening larvicidal, fecundity and longevity effects on malaria vector *Anopheles stephensi*. *Sci. Res. Essays* **8**, (11), 425–431. doi:10.5897/SRE10.373.
32. A. N. Kumar, K. Murugan, and P. Madhiyazhagan (2013). Integration of botanicals and microbials for management of crop and human pests. *Parasitol. Res.* **112**, 313–325.
33. A. Jaganathan, K. Murugan, C. Panneerselvam, P. Madhiyazhagan, D. Dinesh, C. Vadivalagan, A. T. Aziz, B. Chandramohan, U. Suresh, R. Rajaganesh, J. Subramaniam, M. Nicoletti, H. Akon, A. A. Alarfaj, M. A. Munusamy, S. Kumar, and G. Benelli (2016). Earthworm-mediated synthesis of silver nanoparticles: a potent tool against hepatocellular carcinoma, pathogenic bacteria, *Plasmodium* parasites and malaria mosquitoes. *Parasitol. Int.* **65**, 276–284.
34. G. Lamarque (2005). Physicochemical behavior of homogeneous series of acetylated chitosans in aqueous solution: role of various structural parameters. *Biomacromolecules* **6**, (1), 131–142.
35. P. Lertsutthiwong, N. C. How, S. Chandrkrachan, and W. F. Stevens (2002). Effect of chemical treatment on the characteristics of shrimp chitosan. *J. Met. Mater. Miner.* **12**, (1), 11–18.
36. J. Liu, S. Z. Qiao, Q. H. Hu, and G. Q. Lu (2011). Magnetic nanocomposites with mesoporous structures: synthesis and applications. *Small* **7**, (4), 425–443.
37. V. Lobo, A. Phatak, and N. Chandra (2010). Free radicals and functional foods: impact on human health. *Pharmacogn. Rev.* **4**, 118–126.
38. N. A. Luechinger, R. N. Grass, E. K. Athanassiou, and W. J. Stark (2010). Bottom-up fabrication of metal/metal nanocomposites from nanoparticles of immiscible metals. *Chem. Mater.* **22**, (1), 155–160.
39. R. Makowski (1993). Effect of inoculum concentration, temperature, dew period, and plants growth stage on disease of round-leaved mallow and velvetleaf by *Colletotrichum gloeosporioides* f. sp. malvae. *Ecol. Epidemiol.* **83**, 1229–1234.
40. N. K. Mohanpuria and Yadav S. K. Rana (2008). Biosynthesis of nanoparticles: technological concepts and future applications. *J. Nanoparticle Res.* **10**, (3), 507–517.
41. A. Monks, D. Scudiero, P. Skehan, R. Shoemaker, K. Paull, D. Vistica, C. Hose, J. Langley, P. Cronise, A. Vaigro-Wolff, M. Gray-Goodrich, H. Campbell, J. Mayo, and Boyd (1991). Feasibility of high flux anticancer drug screen using a diverse panel of cultured human tumour cell lines. *J. Natl. Cancer Inst.* **83**, 757–766.
42. T. Mosmann (1983). Rapid colorimetric assay for cellular growth and survival: application to proliferation and cytotoxicity assays. *J. Immunol. Methods* **65**, 55–63.
43. R. C. Murdock, L. Braydich-Stolle, A. M. Schrand, J. J. Schlager, and S. M. Hussain (2008). Characterization of nanomaterial dispersion in solution prior to In vitro exposure using dynamic light scattering technique. *Toxicol. Sci.* **101**, (2), 239–253.
44. K. Murugan, R. Vahitha, I. Baruah, and S. C. Das (2003). Integration of botanicals and microbial pesticides for the control of filarial vector, *Culex quinquefasciatus*. *Ann. Med. Entomol.* **12**, 11–23.
45. K. Murugan, G. Benelli, A. Suganya, D. Dinesh, C. Panneerselvam, M. Nicoletti, J. S. Hwang, P. Mahesh Kumar, J. Subramaniam, and U. Suresh (2015). Toxicity of seaweed-synthesized silver nanoparticles against the filariasis vector *Culex quinquefasciatus* and its impact on predation efficiency of the cyclopoid crustacean *Mesocyclops longisetus*. *Parasitol. Res.* **114**, 2243–2253.
46. K. Murugan, J. S. E. Venus, C. Panneerselvam, S. Bedini, B. Conti, M. Nicoletti, S. Kumar Sarkar, J. S. Hwang, J. Subramaniam, P. Madhiyazhagan, P. Mahesh Kumar, D. Dinesh, U. Suresh, and G. Benelli (2015). Biosynthesis, mosquitocidal and antibacterial properties of *Toddalia asiatica* synthesized silver nanoparticles: do they impact predation of guppy *Poecilia reticulata* against the filariasis mosquito *Culex quinquefasciatus*? *Environ. Sci. Pollut. Res.* **22**, (21), 17053–17064.

47. K. Murugan, J. Anitha, D. Dinesh, U. Suresh, R. Rajaganesh, B. Chandramohan, J. Subramaniam, M. Paulpandi, C. Vadivalagan, P. Amuthavalli, L. Wang, J. Hwang, H. Wei, M. Alsalhi, S. Devanesan, S. Kumar, K. Pugazhendy, A. Higuchi, M. Nicoletti, and G. Benelli (2016). Fabrication of nano-mosquitocides using chitosan from crab shells: impact on non- target organisms in the aquatic environment. *Ecotoxicol. Environ. Saf.* **132**, 318–328.
48. R. A. A. Muzzarelli and R. Rochetti (1985). Determination of the degree of deacetylation of chitosan by first derivative ultraviolet spectrophotometry. *J. Carbohydr. Polym.* **5**, 461–472.
49. J. Nirmala and R. Pandian (2015). Extraction and characterization of silver nano particles synthesized using plant extract of *Kedrostis foeditissima* (jacq) Lin. *J. Int. J. Curr. Microbiol. App. Sci.* **4**, (4), 41–47.
50. M. Noginov, G. Zhu, M. Bahoura, J. Adegoke, C. Small, B. A. Ritzo, V. P. Drachav, and V. M. Shalaev (2007). The effect of gain and absorption on surface plasmons in metal nanoparticles. *Appl. Phys. B* **86**, (3), 455–460.
51. W. Olkowski (2001). Larval control of mosquitoes. *Common Sense Pest Control Q.* **17**, 8–18.
52. I. Ostolska and M. Wisniewska (2014). Application of the zeta potential measurements to explanation of colloidal Cr_2O_3 stability mechanism in the presence of the ionic polyamino acids. *Colloid Polym. Sci.* **292**, (10), 2453–2464. doi:10.1007/s00396-014-3276-y.
53. G. F. Paciotti, L. Myer, D. Weinreich, D. Goia, N. Pavel, R. E. McLaughlin, and L. Tamarkin (2004). Colloidal gold: a novel nanoparticle vector for tumor directed drug delivery. *Drug Deliv.* **11**, (3), 169–183.
54. C. Panneerselvam and K. Murugan (2013). Adulticidal, repellent, and ovicidal properties of indigenous plant extracts against the malarial vector, *Anopheles stephensi* (Diptera: Culicidae). *Parasitol. Res.* **112**, (2), 679–692.
55. S. Paula, M. Arianoutsou, D. Kazanis, C. Tavsanoglu, F. Lloret, C. Buhk, F. Ojeda, B. Luna, J. M. Moreno, A. Rodrigo, J. M. Espelta, S. Palacio, B. Fernandez-Santos, P. M. Fernandes, and J. G. Pausas (2009). Fire-related traits for plant species of the Mediterranean Basin. *Ecology* **90**, (5), 1420.
56. B. Pluess, F. C. Tanser, C. Lengeler, B. L. Sharp. (2010) Indoor residual spraying for preventing malaria. Cochrane Database Syst Rev 4: CD006657.
57. L. Qi, Z. Xu, X. Jiang, Y. Li, and M. Wang (2005). Cytotoxic activities of chitosan nanoparticles and copper-loaded nanoparticles. *Bioorg. Med. Chem. Lett.* **15**, 1397.
58. M. Rahman, B. Islam, M. Biswas, and A. H. M. Khurshid Alam (2015). In vitro antioxidant and free radical scavenging activity of different parts of *Tabebuia pallida* growing in Bangladesh. *BMC Res. Notes* **8**, 621. doi:10.1186/s13104-015-1618-6.
59. R. Re, N. Pellegrini, A. Proteggente, A. Pannala, M. Yang, and C. Rice-Evans (1999). Antioxidant activity applying an improved ABTS radical cation decolorization assay. *Free Radic. Biol. Med.* **26**, (9–10), 1231–1237.
60. S. Rodrigues, M. Dionisio, C. R. Lopez, and A. Grenha (2012). Biocompatibility of chitosan carriers with application in drug delivery. *J. Funct. Biomater.* doi:10.3390/jfb3030615.
61. A. P. Rokhade, S. A. Patil, and T. M. Aminabhavi (2007). Synthesis and characterization of semi-interpenetrating microspheres of acrylamide grafted dextran and chitosan for controlled release of acyclovir. *Carbohydr. Polym.* **67**, 605–613.
62. N. Sap-Iam, C. Homklinchan, R. Larpudomlert, W. Warisnoicharoen, A. Sereemaspun, and S. T. Dubas (2010). UV irradiation induced silver nanoparticles as mosquito larvicides. *J. Appl. Sci.* **10**, 31–32.
63. R. Sathyavathi, M. Balamurali Krishna, S. Venugopal Rao, R. Saritha, and Rao D. Narayana (2010). Biosynthesis of silver nanoparticles using *Coriandrum sativum* leaf extract and their application in nonlinear optics. *Adv. Sci. Lett.* **3**, 1–6.
64. K. K. Se and R. Niranjan (2005). Enzymatic production and biological activities of chitosan oligosaccharides (COS): a review. *Carbohydr. Polym.* **62**, 357–368.
65. S. Senthil-Nathan, G. Savitha, D. K. George, A. Narmadha, L. Suganya, and P. G. Chung (2006). Efficacy of *Melia azedarach* L. extract on the malarial vector *Anopheles stephensi* Liston (Diptera: Culicidae). *Biores. Technol.* **97**, 1316–1323.
66. S. Sevda and S. J. McClureb (2004). Potential applications of chitosan in veterinary medicine. *Adv. Drug Deliv. Rev.* **56**, 1467–1480.
67. K. Shimada, K. Fujikawa, K. Yahara, and T. Nakamura (1992). Antioxidative properties of xanthan on the autioxidation of soybean oil in cyclodextrin emulsion. *J. Agric. Food Chem.* **40**, 945–948.

68. A. Singh, D. Jain, M. K. Upadhyay, and N. Khandelwal (2010). Green synthesis of silver nanoparticles using *Argemone mexicana* leaf extract and evaluation of their antimicrobial activities Dig. *J. Nanomater.* **5**, 483–489.
69. B. H. Stuart *Polymer Analysis* (Wiley, New York, 2002).
70. P. Subbiah and B. K. Tyagi (2002). Studies on *Bacillus sphaericus* toxicity related resistance development and biology in the filariasis vector, *Culex quinquefasciatus* (Diptera: Culicidae) form South India. *Appl. Entomol. Zool.* **37**, (3), 365–371.
71. A. A. Sunil, N. M. Nadagouda, and M. Tejraj (2004). Recent advances on chitosan-based micro and nanoparticles in drug delivery. *J. Controlled Release* **100**, 5–28.
72. U. Suresh, K. Murugan, G. Benelli, M. Nicoletti, D. R. Barnard, C. Panneerselvam, P. Mahesh Kumar, J. Subramaniam, D. Dinesh, and B. Chandramohan (2015). Tackling the growing threat of dengue: *Phyllanthus niruri*-mediated synthesis of silver nanoparticles and their mosquitocidal properties against the dengue vector *Aedes aegypti* (Diptera: Culicidae). *Parasitol. Res.* **114**, 1551–1562.
73. D. K. Tiwari, J. Behari, and P. Sen (2008). Time and dose-dependent antimicrobial potential of Ag nanoparticles synthesized by top-down approach. *Curr. Sci.* **95**, (5), 647–655.
74. W. I. Tong, W. F. Dong, C. Y. GAo, and H. Mohwald (2005). Charge-controlled permeability of polyelectrolyte microcapsules. *J. Phys. Chem. B* **109**, 13159–13165.
75. S. T. Trang and N. D. B. Huynh (2015). Physicochemical properties and antioxidant activity of chitin and chitosan prepared from pacific white shrimp waste. *Int. J. Carbohydr. Chem.* doi:10.1155/2015/706259.
76. T. S. Trung, W. W. Thein-Han, N. T. Qui, C. H. Ng, and W. F. Stevens (2006). Functional characteristics of shrimp chitosan and its membranes as affected by the degree of deacetylation. *Bioresour. Technol.* **97**, 659–663.
77. WHO (2016) Malaria Fact sheet, Updated January 2016.
78. P. Yanez-Sedeno and J. M. Pingarron (2005). Gold nanoparticle-based electrochemical biosensors. *Anal. Bioanal. Chem.* **382**, (4), 884–886.
79. Q. Yao, P. Nooeaid, J. A. Roether, Y. Dong, Q. Zhang, and A. R. Boccaccini (2013). Bioglass®-based scaffolds incorporating polycaprolactone and chitosan coatings for controlled vancomycin delivery. *Ceram. Int.* **39**, 7517.
80. C. P. W. Zebitz (1984). Effects of some crude and azadirachtin enriched neem *Azadirachita indica* seed kernel extracts on larvae of *Aedes aegypti*. *Entomol. Exp. Appl.* **35**, 11–14.
81. C. P. W. Zebitz (1986). Effects of three neem seed kernel extracts and azadirachtin on larvae of different mosquito species. *J. Appl. Entomol.* **102**, 455–463.
82. B. Zebli, A. S. Susha, G. B. Sukhorukov, A. L. Rogach, and W. J. Parak (2005). Magnetic targeting and cellular uptake of polymer microcapsules simultaneously functionalized with magnetic and luminescent nanocrystals. *Langmuir* **21**, (10), 4262–4265.